RSC Advances

PAPER

View Article Online
View Journal | View Issue



Cite this: *RSC Adv.*, 2017, **7**, 10782



# Monte Carlo track chemistry simulations of the radiolysis of water induced by the recoil ions of the $^{10}B(n,\alpha)^{7}Li$ nuclear reaction. 1. Calculation of the yields of primary species up to 350 °C

Muhammad Mainul Islam,[a] Phantira Lertnaisat,[b] Jintana Meesungnoen,[a] Sunuchakan Sanguanmith,[a] Jean-Paul Jay-Gerin,*[a] Yosuke Katsumura,†*[b] Satoru Mukai,[c] Ryuji Umehara,[d] Yuichi Shimizu[d] and Masashi Suzuki[c]

Monte Carlo track chemistry simulations were carried out to predict the yields (*G*-values) of all primary radical and molecular species produced in the radiolysis of pure, neutral water and 0.4 M sulfuric acid aqueous solutions by the recoil ions of the $^{10}B(n,\alpha)^{7}Li$ nuclear reaction as a function of temperature from 25 to 350 °C. The calculations were performed individually for 1.47 MeV α-particles and 0.84 MeV lithium nuclei with "dose-average" linear energy transfer (LET) values of ~196 and 225 eV nm$^{-1}$ at 25 °C, respectively. The overall yields were calculated by summing the *G*-values for each recoil ion weighted by its fraction of the total energy absorbed. In the calculations, the actual effective charges carried by the two helium and lithium ions (due to charge exchange effects) were taken into account and the (small) contribution of the 0.478 MeV γ-ray, also released from the $^{10}B(n,\alpha)^{7}Li$ reaction, was neglected. Compared with data obtained for low-LET radiation ($^{60}Co$ γ-rays or fast electrons), our computed yields for the $^{10}B(n,\alpha)^{7}Li$ radiolysis of neutral deaerated water showed essentially similar temperature dependence over the range of temperatures studied, but with lower values for yields of free radicals and higher values for molecular yields. This general trend is a reflection of the high-LET character of the $^{10}B(n,\alpha)^{7}Li$ recoil ions. Overall, the simulation results agreed well with existing estimates at 20 and 289 °C. For deaerated 0.4 M $H_2SO_4$ solutions, reasonable agreement between experiment and simulation was also found at room temperature. Nevertheless, more experimental data for both neutral and acidic solutions would be needed to better describe the dependence of radiolytic yields on temperature and to test our modeling calculations more thoroughly. Moreover, measurements of the ($e_{aq}^{-}$ + $e_{aq}^{-}$) reaction rate constant in near-neutral water would help us to determine whether the predicted non-monotonic inflections above ~150 °C in $G(H_2)$ and $G(H_2O_2)$ are confirmed.

Received 22nd December 2016
Accepted 2nd February 2017

DOI: 10.1039/c6ra28586d

rsc.li/rsc-advances

## 1. Introduction

Boron-10 is one of the stable isotopes of boron with a natural abundance of ~20%. It is known to exhibit a high propensity to absorb thermal neutrons with a neutron-capture cross-section of 3835 barns (1 barn = $10^{-28}$ m$^2$), which is about six times greater than that of uranium-235 and three orders of magnitude greater than that of the nuclei of living tissues.[1] On absorption of a slow neutron, a fission reaction occurs with the release of two energetic heavy ions: an α-particle (1.47 MeV) and, in ~94% of all reactions, a $^{7}Li^{3+}$ nucleus in its first excited state (0.84 MeV) which quickly returns to its ground state (half-life of ~$10^{-13}$ s) by releasing a low-energy γ-ray (478 keV).[2] These heavy charged particles have path lengths in the range of ~5–8 μm in water or biological tissues and exhibit high linear energy transfer (LET, or energy loss per unit path length $-dE/dx$, in units of eV nm$^{-1}$) characteristics, as shown in Fig. 1.[3,4] Because of this high energy deposition to the surrounding environment and the α and Li recoils' short travel distances, which are typically of the order of a cell diameter, the $^{10}B(n,\alpha)^{7}Li$ nuclear reaction has been used in clinical studies of biochemically targeted radiotherapies for cancer

[a]*Département de Médecine Nucléaire et de Radiobiologie, Faculté de Médecine et des Sciences de la Santé, Université de Sherbrooke, Sherbrooke, Québec, J1H 5N4, Canada. E-mail: jean-paul.jay-gerin@USherbrooke.ca*

[b]*Department of Nuclear Engineering and Management, School of Engineering, University of Tokyo, 7-3-1 Hongo, Bunkyo-ku, Tokyo 113-8686, Japan. E-mail: katsu@n.t.u-tokyo.ac.jp*

[c]*Nuclear Chemistry Engineering, Nuclear Environment R&D Department, Nuclear Development Corporation, 622-12 Funaishikawa, Tokai-mura, Ibaraki 319-111, Japan*

[d]*Water Chemistry Technology Group, Nuclear Energy Systems Headquarters, Mitsubishi Heavy Industries Ltd., 1-1-1 Wadasaki-cho, Hyogo-ku, Kobe 652-8585, Japan*

† Present address: Japan Radioisotope Association, Honkomagome 2-28-45, Bunkyo-ku, Tokyo 113-8941, Japan.

treatment known as "boron neutron capture therapy" (BNCT).[1,5]

BNCT is a potentially ideal radiotherapy modality for glioblastoma, which is a type of brain tumor that is rarely removed surgically. When a cancer cell is allowed to take up preferentially a sufficient concentration of $^{10}B$, it can be selectively irradiated by the very densely ionizing ion recoils from the $^{10}B(n,\alpha)^{7}Li$ reaction without damaging the surrounding normal tissue. This basic idea was first proposed by Locher in 1936,[6] shortly after the discovery of the neutron by Chadwick.[7] Interest in BNCT was spurred by Kruger's study in 1940, who reported a low transplantation efficiency for tumors treated by BNCT *in vitro* and subsequently implanted in mice.[8,9] Although the full clinical application of BNCT presents several difficulties, including the inadequate selectivity and toxicity of $^{10}B$ delivery agents and the poor distribution of neutron flux, clinical trials of BNCT are still under way and new neutron irradiation facilities continue to be developed in Japan, the United States, Finland, and several other countries.[1,5,10–12]

Apart from BNCT, the unique properties of boron-10 have also been extensively applied in the field of nuclear industry. For example, boron carbide ($B_4C$), enriched in $^{10}B$, is used as a control-rod material (neutron absorber) in boiling water reactors (BWRs). In addition, boron as boric acid ($H_3BO_3$) is generally added as a water-soluble neutron poison in the primary coolant of pressurized water reactors (PWRs) to control the neutron flux and the reactivity in the core.[13–16] However, recoil ions arising from the $^{10}B(n,\alpha)^{7}Li$ reaction act as sources of high-LET radiation in the primary coolant of PWRs, thereby leading to the formation of oxidizing species, such as hydrogen peroxide and oxygen, due to the radiolysis of water.[17,18]

The radiolysis of water is closely linked to the corrosion of structural materials. Water, which is used as the neutron moderator and the reactor coolant, is unavoidably exposed to extreme conditions of high temperature (~275–325 °C), pressure (~7–15 MPa), and intense mixed neutron and β–γ radiation fields (which have characteristically different LET values). Under these conditions, the radiolysis of water results in the formation of free radical ($e_{aq}^-$, $H^\bullet$, $^\bullet OH$, and $HO_2^\bullet/O_2^{\bullet-}$) and molecular ($H_2$, $H_2O_2$, and $O_2$) species which alter the chemical environment of the coolant.[18–20] The presence of the oxidizing species $H_2O_2$ and $O_2$ can significantly increase the corrosion potential of coolant water in BWRs.[16,21,22] In PWRs, the presence of boron-10 results in high-LET recoil ions and complicates the radiolytic process. Although $^{10}B$ has been widely studied both in nuclear technology and clinical research, little attention has been devoted to $^{10}B$-induced reactions. In particular, data on the formation of primary products and their yields (*G*-values) for $^{10}B(n,\alpha)^{7}Li$ recoil irradiation of neutral water are scarce and uncertain.[15,19] In fact, the only reported measurements at room temperature were made in acid (0.4 M $H_2SO_4$) solution.[23–25] Similarly, the *G*-values at reactor temperatures are not well known. To the best of our knowledge, there is only one report[19] that estimated a complete set of water decomposition yields induced by the $^{10}B(n,\alpha)^{7}Li$ reaction at 289 °C.

Understanding the radiation chemistry of the coolant water in reactors is important for maintaining the proper chemical environment that will minimize the degradation of materials. Recently, computer simulations have played a substantial role in evaluating the concentrations of oxidizing species produced from coolant-water radiolysis, which is difficult to observe directly because of the extreme operating conditions involved. In this current work, Monte Carlo track chemistry simulations were undertaken to predict the *G*-values for the various primary radical and molecular products formed from the radiolysis of pure, neutral water and 0.4 M $H_2SO_4$ aqueous solutions by the $^{10}B(n,\alpha)^{7}Li$ reaction as a function of temperature from 25 to 350 °C.

The paper is organized as follows. The main features of our simulation approach are given in the next section. Sections 3 and 4 present, respectively, the results of our simulations of the $^{10}B(n,\alpha)^{7}Li$ radiolysis of water at neutral pH and of 0.4 M $H_2SO_4$ aqueous solutions at 25 °C and as a function of temperature up to 350 °C, and their discussion. Conclusions are drawn in the final section.

A brief preliminary report of this work has been presented elsewhere.[26]

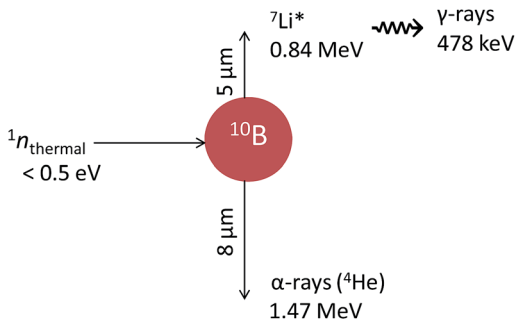


Fig. 1 Scheme of the nuclear reaction resulting from the low-energy (<0.5 eV) thermal neutron capture by a $^{10}B$ atom. After absorption, 94% of the reactions leave the $^{7}Li$ ion in its first excited state ($^{7}Li^*$) which rapidly de-excites to the ground state by releasing a 478 keV γ-ray. For the remaining 6% of the reactions, the $^{7}Li$ ion is left directly in its ground state resulting in the emission of a 1.78 MeV α-particle and a 1.02 MeV $^{7}Li$ ion. Note that the $^{4}He$ and $^{7}Li$ recoil ions are in opposite directions (*i.e.*, at a 180° angle), away from the site of the compound nucleus, and hence they form one straight track.

## 2. Monte Carlo track chemistry simulations

The entire sequence of events generated in the radiolysis of liquid water by $^{10}B(n,\alpha)^{7}Li$ recoil ions was modeled using our Monte Carlo track chemistry simulation code called IONLYS-IRT. This computer program simulates, in a 3D geometrical environment, the highly nonhomogeneous distribution of reactive species initially produced by the absorption of incident radiation and all of the energetic secondary electrons, as well as the subsequent diffusion and chemical reactions of these species. A detailed description of the current version of the code at both ambient and elevated temperatures and under low- and

high-LET irradiation conditions has been reported previously.[27–30] In brief, the IONLYS step-by-step simulation program models all of the events of the early "physical" and "physico-chemical" stages[31] of radiation action up to ~1 ps in the track development. The complex, highly nonhomogeneous spatial distribution of reactants formed at the end of the physico-chemical stage [$e_{aq}^-$, $H^+$, $OH^-$, $H^\bullet$, $^\bullet OH$, $H_2$, $H_2O_2$, $HO_2^\bullet/O_2^{\bullet-}$, $^\bullet O(^3P)$, $O(^1D)$, $O_2$,…], which is provided as an output of the IONLYS program, is then used directly as the starting point for the subsequent "nonhomogeneous chemical" stage[31] (typically, from ~1 ps to the μs time scale at 25 °C). This third stage, during which the different radiolytic species diffuse randomly at rates determined by their diffusion coefficients and react with one another (or with dissolved solutes, if any) until all track processes are complete, is covered by our IRT program. This program employs the "independent reaction times" (IRT) method,[32–34] a computationally efficient stochastic simulation technique that is used to simulate reaction times without having to follow the trajectories of the diffusing species. The IRT method relies on the approximation that the reaction time of each pair of reactants is independent of the presence of other reactants in the system. Its ability to give accurate time-dependent chemical yields under different irradiation conditions has been well validated by comparison with full random flights (or step-by-step) Monte Carlo simulations, which do follow the reactant trajectories in detail.[35,36] This IRT program can also be used to efficiently describe the reactions that occur in the bulk solution during the "homogeneous chemical" stage,[31] *i.e.*, in the time domain beyond a few microseconds. The model assumptions and procedures employed to carry out the Monte Carlo simulations of the radiolysis of aqueous 0.4 M $H_2SO_4$ solutions (pH ~ 0.46) with IONLYS-IRT have already been given.[37,38]

In the current version of IONLYS-IRT, we used the self-consistent radiolysis database, including rate constants and diffusion coefficients, recently compiled by Elliot and Bartels.[20] This new database provides recommendations for the best values to use in high-temperature modeling of water radiolysis over the range of 20–350 °C.

Pre-simulations were performed using the SRIM simulation program[39] to calculate 1000 tracks of 1.47 MeV α-particles and 0.84 MeV lithium nuclei emitted from the $^{10}B(n,\alpha)^7Li$ reaction, and the energies and LET values of the 2 recoil ions as a function of penetration depth in water (Fig. 2). As shown, the initial LETs of helium and lithium ions were ~193 and 304 eV $nm^{-1}$, respectively. The LET of 1.47 MeV $^4He^{2+}$ ions calculated using our Monte Carlo simulations agreed very well with the SRIM simulation results. Since the SRIM program incorporates the change of charge state of the moving ion as it goes into and through the target (due to the effects of electron capture and loss by the ion), this agreement indicates that the helium ion, when it travels with this energy, is fully stripped of its electrons. However, for 0.84 MeV $^7Li^{3+}$ ions, our calculations gave a LET which is more than twice the expected value. This difference was explained as being caused by a change in the charge state of the lithium ion, which always acts to reduce its LET relative to the LET of the bare nucleus. Our Monte Carlo simulations were

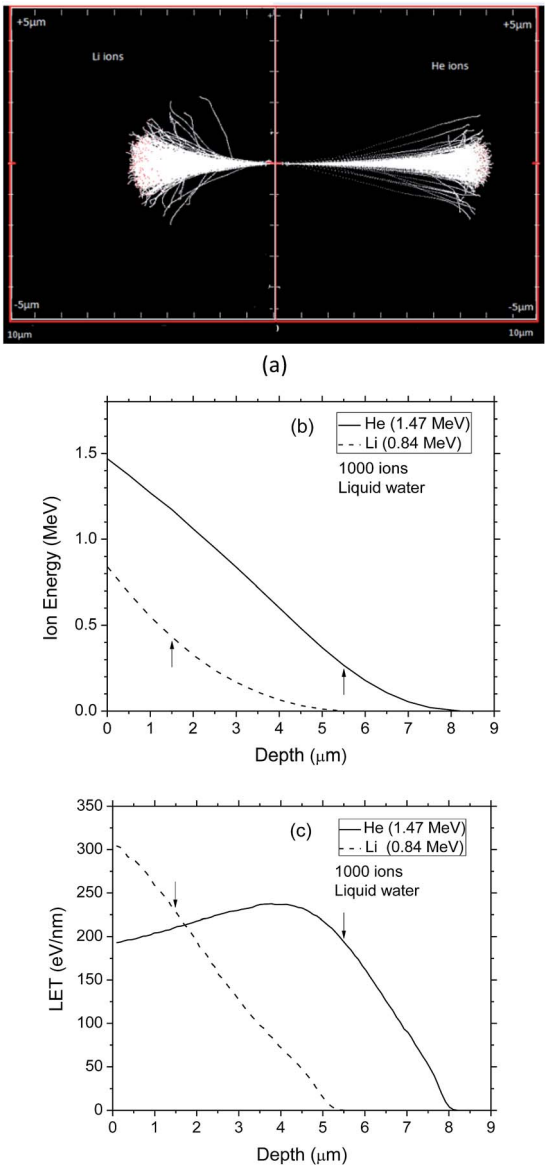


Fig. 2 SRIM simulation of the penetration of the recoil helium and lithium ions of the $^{10}B(n,\alpha)^7Li$ reaction into liquid water at room temperature: (a) simulated ion trajectories; (b) and (c) variations of the energy and LET of the two ions as a function of penetration depth, respectively (the points selected in this study are indicated by arrows). Total ions calculated: 1000.

used to calculate the "effective charge" ($Z^*$) of a 0.84 MeV lithium ion in water that was required to reproduce the SRIM LET value of 304 eV $nm^{-1}$. A value very close to +2 (instead of +3) was actually obtained, clearly indicating a partial neutralization of the lithium ion at this energy.

The above results confirm the importance of making charge-state calculations for each recoil ion in this study. In this work, however, to avoid complexity arising from energy-dependent charge exchange processes, simulations were performed under the simplifying approximation that the energies of the two recoil ions remained constant when passing through the water medium. These constant average energy values $\overline{E_{He}}$ and

$\overline{E_{Li}}$ were chosen according to the following procedure: (1) Watt's compilation of quantities for radiation dosimetry in liquid water[3] was first used to determine the "dose-average" LET values for both 1.47 MeV helium and 0.84 MeV lithium ions. The values thus obtained were ~196 and 225 eV nm$^{-1}$, respectively; (2) using Fig. 2(c), these two LET values were then related to the corresponding penetration depths of the two recoil ions in water, namely, ~5.5 and 1.5 μm, respectively; and (3) $\overline{E_{He}}$ and $\overline{E_{Li}}$ were finally deduced from Fig. 2(b) as being equal to the energies of the two ions at these penetration depths, namely, ~0.3 and 0.4 MeV, respectively. Once these two energies known, the actual effective charges carried by the two helium and lithium ions having these energies were determined as described above by using our Monte Carlo simulations and by adjusting $Z^*$ so as to reproduce the expected LET values. $Z^*_{He}$ and $Z^*_{Li}$ were found to be about +1.6 and +1.7, respectively.

All calculations were performed by simulating short (typically, ~1–5 μm) ion track segments, over which the energy and LET of the ion are well defined and remain nearly constant. Such model calculations thus gave "track segment" yields[40] at a well defined LET. The number of individual ion "histories" (usually ~2–100, depending on the irradiating ion and energy) was chosen to ensure only small statistical fluctuations in the computed averages of chemical yields, while keeping acceptable computer time limits.

Finally, the yields of primary free radical or molecular products of water radiolysis induced by the recoil ions of the nuclear reaction $^{10}$B(n,α)$^7$Li were calculated by summing the $G$-values for each recoil ion (obtained from our Monte Carlo simulations) weighted by its fraction of the total energy absorbed according to[38,41]

$$G(X_i) = \frac{G(X_i)_{He} E_{He} + G(X_i)_{Li} E_{Li}}{E_T}, \quad (1)$$

where $G(X_i)_{He}$ and $G(X_i)_{Li}$ are the yields of species $X_i$ associated with the recoil helium and lithium ions, respectively, and $E_T = E_{He} + E_{Li}$ is the sum of the initial energies of the ion products of the reaction (*i.e.*, 2.31 MeV).

Absorption of the accompanying 0.478 MeV γ-ray in the aqueous solution (see Fig. 1) is small in our area of interest. Indeed, the range of an electron of this energy is ~1 mm in liquid water at 25 °C;[42] this is more than 100 times larger than the penetration ranges of the He and Li ions, which are only 5–8 μm. Thus, its contribution to the overall chemical reaction was neglected in this study.

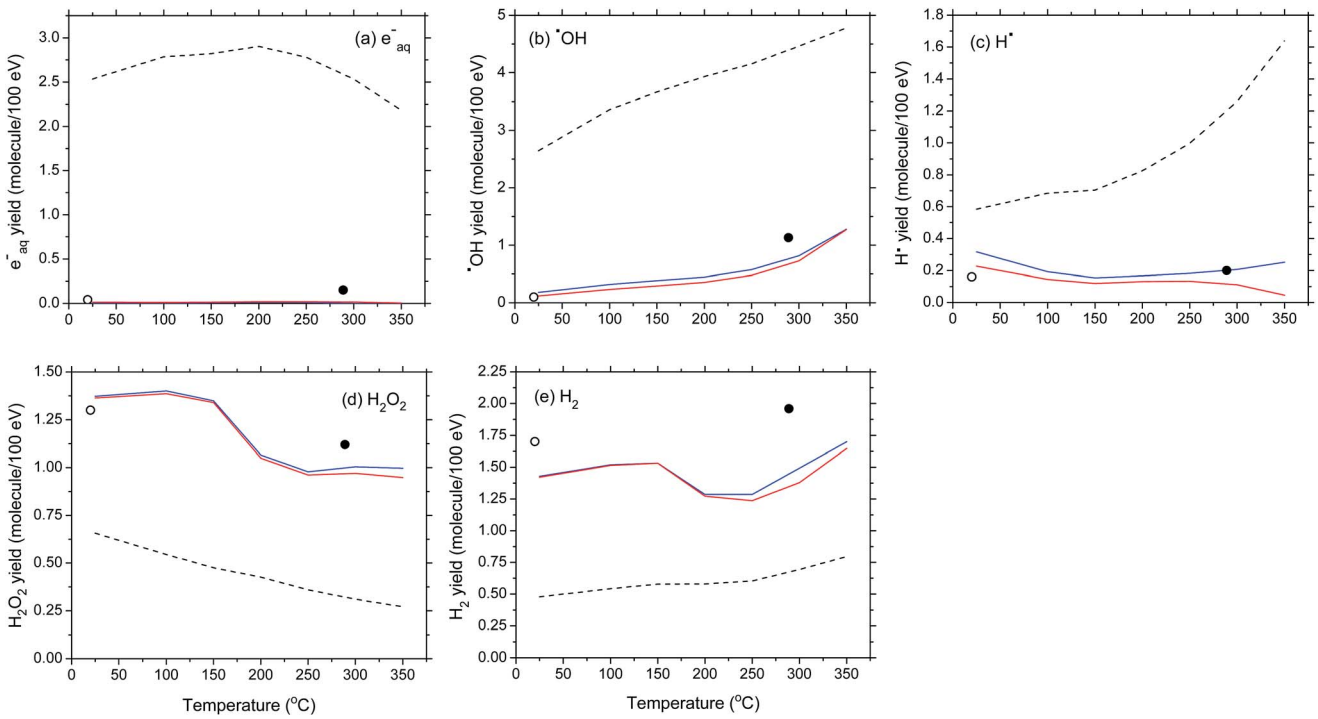


Fig. 3 $G$-values (in molecule per 100 eV) for the $^{10}$B(n,α)$^7$Li radiolysis of pure, deaerated liquid water as a function of temperature in the range of 25–350 °C: (a) $G(e_{aq}^-)$; (b) $G(^{\bullet}OH)$; (c) $G(H^{\bullet})$; (d) $G(H_2O_2)$; and (e) $G(H_2)$. Our simulated results, obtained at $10^{-7}$ and $10^{-6}$ s, are shown as solid, blue and red lines, respectively. Symbols are the water decomposition yields induced by the $^{10}$B(n,α)$^7$Li reaction estimated by Cohen (ref. 15) at 20 °C (based on the approximate relationship between LET and $G$-values given in Fig. 5.3 of Allen (ref. 43), using an average initial LET of 240 eV nm$^{-1}$) (○) and by Christensen (ref. 19) at 289 °C (●). The primary (or "escape") yields for the low-LET (~0.3 eV nm$^{-1}$) radiolysis of water (ref. 29) obtained using our previously calculated spur lifetimes between 25–350 °C (ref. 44) are also given (black dashed lines) for comparison purposes. Note that all yield curves shown in this figure were obtained under exactly the same conditions as in ref. 29 as far as the temperature dependences of the different parameters intervening in the early physicochemical stage (*e.g.*, the electron thermalization distance – called $r_{th}$ in ref. 29) and in the subsequent chemical stage [*e.g.*, the ($e_{aq}^- + e_{aq}^-$) reaction rate constant, represented by the non-Arrhenius black dashed line $k = k_a$ in Fig. 4(a)] of the radiolysis are concerned.

Throughout this paper, *G*-values are quoted in units of molecules formed or consumed per 100 eV of radiation energy absorbed. For conversion into SI units, 1 molecule/100 eV = 0.10364 μmol $J^{-1}$.

## 3. Results and discussion

The temperature dependences of our computed yields of $e_{aq}^-$, $^{\bullet}OH$, $H^{\bullet}$, $H_2O_2$, and $H_2$ in pure, deaerated liquid water irradiated by the $^{10}B(n,\alpha)^7Li$ recoil ions from ambient up to 350 °C are shown in Fig. 3 along with estimated *G*-values at 20 °C (ref. 15) and 289 °C.[19] For the sake of comparison, our *G*-values were calculated at two different times, namely $10^{-7}$ and $10^{-6}$ s after energy deposition at all temperatures (solid, blue and red lines shown in Fig. 3, respectively). Compared with the data obtained for low-LET radiation (γ-rays from $^{60}Co$ or fast electrons), our computed yields for $^{10}B(n,\alpha)^7Li$ recoil irradiation show essentially similar temperature dependences over the range of temperatures studied, but with much lower values for yields of free radicals and higher values for molecular yields. This is particularly true for the yields of $e_{aq}^-$ and $H^{\bullet}$ atoms, which remain extremely small at the microsecond time scale even at high temperatures [Fig. 3(a) and (c)]. This general trend is a result of the high-LET character of the $^{10}B(n,\alpha)^7Li$ recoil ions. Indeed, upon increasing the LET of the radiation, there is an increased intervention of radical–radical reactions as the local concentrations of radicals along the radiation tracks are high and many radical interactions occur before the products can escape into the bulk solution. This allows fewer radicals to escape combination and recombination reactions during the expansion of tracks and in turn leads to the formation of more molecular products.[28]

A striking feature of our simulated results is the marked downward inflection that is observed above ~150 °C in the yields of $H_2$ and $H_2O_2$. This is in contrast to the corresponding estimates of Christensen[19] at 289 °C, which seem to indicate a rather monotonic variation of $G(H_2)$ [Fig. 3(e)] and $G(H_2O_2)$ [Fig. 3(d)] with temperature. Similar non-monotonic behavior in the temperature dependence of the yields of primary products in low-[29,45,46] and high-[47,48] LET irradiated water has already been predicted, and is due to the fact that the rate constant for the bimolecular self-reaction of the hydrated electron ($k_2$):

$$e_{aq}^- + e_{aq}^- (+2H_2O) \rightarrow H_2 + 2OH^- \quad (2)$$

drops sharply between ~150 and 200 °C.[20] This non-Arrhenius behavior of reaction (2) above ~150 °C readily explains the sharp decrease in $H_2$ yields in Fig. 3(e). Moreover, as a consequence of the drop in $k_2$, more and more $e_{aq}^-$ are available as the temperature increases to either react in other intra-track reactions, such that[20]

$$e_{aq}^- + {}^{\bullet}OH \rightarrow OH^- (k_3 = 3.34 \times 10^{10}\ M^{-1}\ s^{-1}, 20\ ^{\circ}C), \quad (3)$$

or escape into the bulk solution. As hydrogen peroxide is formed predominantly by the reaction[20]

$$^{\bullet}OH + {}^{\bullet}OH \rightarrow H_2O_2 (k_4 = 4.54 \times 10^9\ M^{-1}\ s^{-1}, 20\ ^{\circ}C), \quad (4)$$

the increased occurrence of reaction (3) above 150 °C also leads to a downward inflection in $G(H_2O_2)$, as shown in Fig. 3(d).

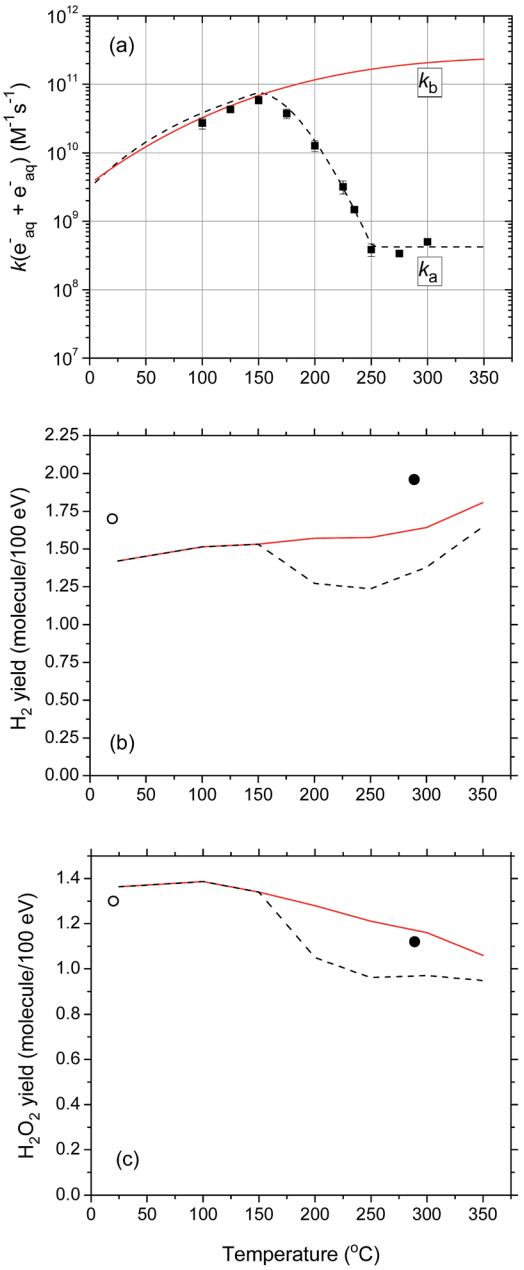


Fig. 4 (a) Rate constant for the self-reaction of two hydrated electrons as a function of temperature (ref. 49). The black dashed line (denoted $k_a$) shows the ($e_{aq}^- + e_{aq}^-$) reaction rate constant measured under alkaline conditions (ref. 20). The symbols (■) are experimental data. The red solid line (denoted $k_b$) shows the ($e_{aq}^- + e_{aq}^-$) reaction rate constant obtained by using an Arrhenius extrapolation procedure above ~150 °C (ref. 50–52). (b) and (c) The red solid lines show our Monte Carlo simulation results for $G(H_2)$ and $G(H_2O_2)$ (in molecule per 100 eV), at $10^{-6}$ s, as a function of temperature, when $k_b$ was used. A comparison is made with the corresponding yields of $H_2$ and $H_2O_2$ obtained when $k_a$ was used [represented here by the black dashed lines, which are the same as the red solid lines in Fig. 3(e) and (d)]. The symbols (○) (ref. 15) and (●) (ref. 19) are the same as in Fig. 3(e) and (d).

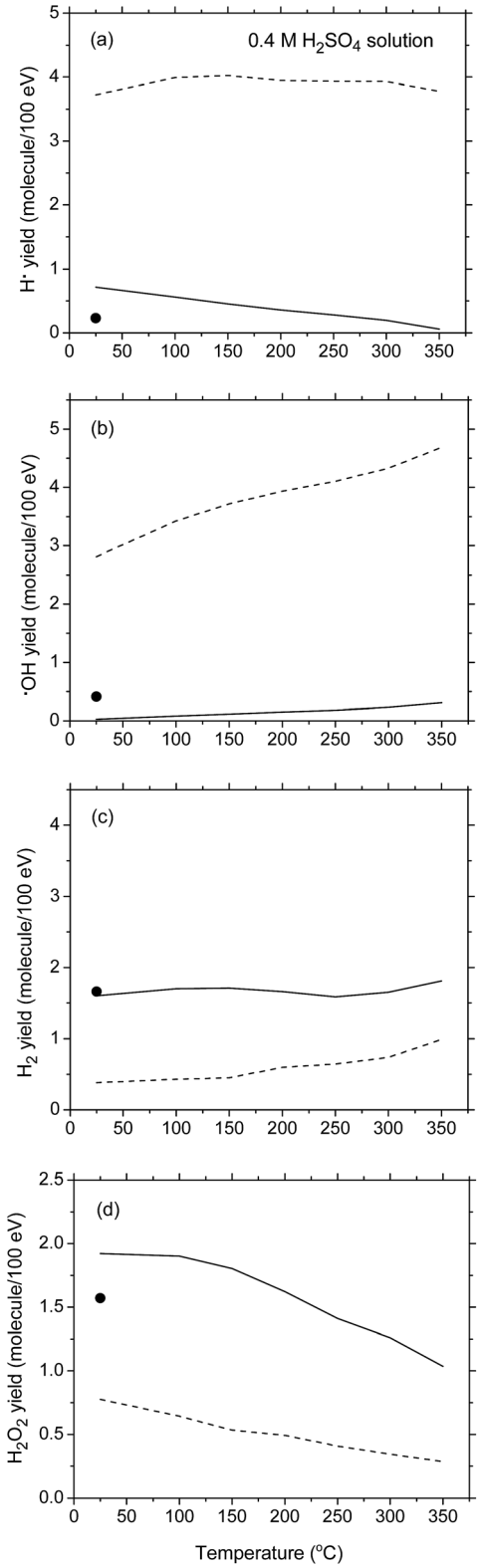


Fig. 5 *G*-values (in molecule per 100 eV) for the $^{10}B(n,\alpha)^7Li$ radiolysis of deaerated 0.4 M $H_2SO_4$ aqueous solutions (pH 0.46 at 25 °C) as a function of temperature in the range of 25–350 °C. Note that, at this high concentration of $H_2SO_4$, the $H^+$ ions very rapidly (<$10^{-9}$ s) scavenge most, if not all, of the $e_{aq}^-$ radicals in the tracks to form $H^{\bullet}$ atoms (ref. 37). Note also that, in our simulations, the direct action of ionizing radiation on the sulfuric acid anions (mainly $HSO_4^-$) has been neglected. The solid curves represent the results of our Monte Carlo simulations for (a) $G(H^{\bullet})$, (b) $G(^{\bullet}OH)$, (c) $G(H_2)$, and (d) $G(H_2O_2)$ at $10^{-6}$ s after the initial energy deposition. The yields of primary species induced by the $^{10}B(n,\alpha)^7Li$ reaction measured by Barr and Schuler (ref. 23) in acidic solutions at 25 °C are given by (●). The primary (or "escape") yields for the low-LET (~0.3 eV $nm^{-1}$) radiolysis of 0.4 M $H_2SO_4$ aqueous solutions (ref. 53) obtained from our previously calculated spur lifetimes between 25–350 °C (ref. 44) are also shown (dashed lines) for the sake of comparison. Finally, in all calculations, the reaction of the $H^{\bullet}$ atom with water: $H^{\bullet} + H_2O \rightarrow H_2 + {}^{\bullet}OH$ was assumed to follow an Arrhenius temperature dependence over the 25–350 °C range studied, with a rate constant of $4.6 \times 10^{-5}$ $M^{-1}$ $s^{-1}$ at 25 °C and $10^4$ $M^{-1}$ $s^{-1}$ at 300 °C, in agreement with recent muon spin spectroscopy experiments using muon as an analogue of a hydrogen atom (ref. 54).

In connection with these predicted non-monotonic variations of $G(H_2)$ and $G(H_2O_2)$, we should briefly mention here the current controversy concerning the temperature dependence of $k_2$ (Fig. 4). In this work, we adopted the values of $k_2$, including the drop between 150 and 200 °C, recommended by Elliot and Bartels[20] as the "best values to use to model water radiolysis at temperatures up to 350 °C" [represented by the black dashed line, denoted $k_a$, in Fig. 4(a)]. However, this drop in $k_2$ has been measured only under alkaline conditions. Its applicability to neutral or slightly acidic (as the pH of water at 150–200 °C is about 5.7–6)[15] solution remains uncertain because it could be a function of the pH of the solution.[50]

Until recently, most computer modelers of the radiolysis of water at elevated temperatures have employed, in neutral solution, an Arrhenius extrapolation of the values of $k_2$ below 150 °C to 200–350 °C, as proposed previously by Elliot[50] and Stuart *et al.*,[51] and recently by Hatomoto *et al.*[52] This approach assumes that such an abrupt change in $k_2$ does not occur and that reaction (2) is diffusion controlled at temperatures greater than 150 °C. This assumption was originally justified by the good agreement between models and experiments.[45,46]

To show the sensitivity of $G(H_2)$ and $G(H_2O_2)$ to $k_2$, our simulations were carried out for the temperature dependence of $k_2$ obtained by using an Arrhenius extrapolation procedure above ~150 °C (ref. 49–52) [represented by the red solid line, denoted $k_b$, in Fig. 4(a)]. The red solid lines in Fig. 4(b) and (c) display our calculated $H_2$ and $H_2O_2$ yields at $10^{-6}$ s after the ionizing event over the temperature range of 25–350 °C. A comparison with our results obtained using the temperature dependence of $k_2$ measured in alkaline water ($k_a$) [black dashed lines in Fig. 4(b) and (c)] clearly indicates that $G(H_2)$ and $G(H_2O_2)$ are strongly affected by the choice of $k_2$. In particular, the sharp downward inflections predicted for $G(H_2)$ and $G(H_2O_2)$ above ~150 °C no longer appear. Considering the importance of the self-reaction of $e_{aq}^-$ in high-temperature water radiolysis, further measurements of its rate constant in near-neutral water are obviously highly desirable.

Turning now to the $^{10}B(n,\alpha)^7Li$ radiolysis of deaerated 0.4 M sulfuric acid aqueous solutions, we present in Fig. 5 the results of our Monte Carlo simulations showing the variations of the *G*-values for $H^{\bullet}$ (considering the conversion of $e_{aq}^-$ to $H^{\bullet}$ in the tracks in acidic solution),[55] $^{\bullet}OH$, $H_2O_2$, and $H_2$ (at $10^{-6}$ s) as a function of temperature over the range of 25–350 °C. As can be

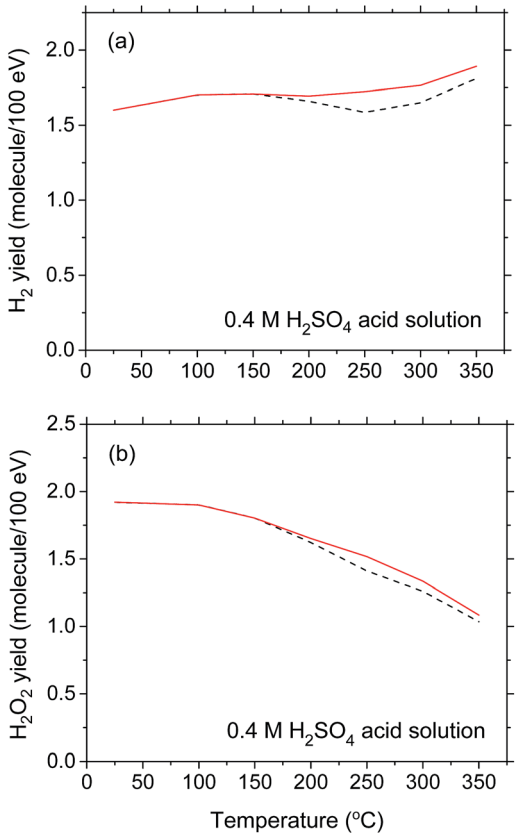


Fig. 6 Yields of $H_2$ (panel a) and $H_2O_2$ (panel b) (in molecule per 100 eV) formed during the $^{10}B(n,\alpha)^7Li$ radiolysis of deaerated 0.4 M $H_2SO_4$ aqueous solutions as a function of temperature over the range of 25–350 °C. The black dashed lines show our Monte Carlo simulation results for $G(H_2)$ and $G(H_2O_2)$ at $10^{-6}$ s when the $(e_{aq}^- + e_{aq}^-)$ reaction rate constant $k_2 = k_a$ [see Fig. 4(a)] was used (note that these curves are the same as the lines in Fig. 5(c) and (d)). A comparison is made with the corresponding yields of $H_2$ and $H_2O_2$ obtained when $k_2 = k_b$ [see Fig. 4(a)] was used (represented by the red solid lines).

seen, the simulations agree reasonably well with the experimental data of Barr and Schuler[23] at 25 °C, which are also shown in the figure for the sake of comparison. Compared with the primary (or "escape") yield data obtained for low-LET radiation ($^{60}Co$ γ-rays or fast electrons) (shown as dashed lines in Fig. 5), it is seen that, as in neutral water, our computed *G*-values for the $^{10}B(n,\alpha)^7Li$ radiolysis of deaerated 0.4 M $H_2SO_4$ aqueous solutions show essentially similar temperature dependences over the 25–350 °C temperature range studied. The same general trend is observed, but with much lower values for yields of radical species and higher values for molecular yields, reflecting again the high-LET character of the $^{10}B(n,\alpha)^7Li$ recoil ions.

For the sake of completeness, we show in Fig. 6 the sensitivity of $G(H_2)$ and $G(H_2O_2)$ to the temperature dependence for the $(e_{aq}^- + e_{aq}^-)$ reaction rate constant $k_2$ chosen in the simulations. Compared to the results obtained in near-neutral water and shown in Fig. 4(b) and (c), the choice of $k_2$ [namely, $k_a$ or $k_b$ in Fig. 4(a)] in acidic solution is relatively unimportant. Indeed, as can be seen from Fig. 6(a) and (b), the $H_2$ and $H_2O_2$ yield (red solid) curves obtained using $k_2 = k_a$ differ only slightly from the corresponding (black dashed) curves calculated for $k_2 = k_b$ and the downward inflections predicted for $G(H_2)$ and $G(H_2O_2)$ above ~150 °C are practically no longer apparent. This is easily understandable since in 0.4 M $H_2SO_4$ solutions, hydrated electrons are very rapidly ($<10^{-9}$ s) transformed into $H^\bullet$ atoms in the tracks,[37] thereby making reaction (2) quickly inoperative in contributing to these yields whatever the temperature. Removal of this reaction thus prevents the possibility of observing any clear difference in the temperature dependence of $G(H_2)$ and $G(H_2O_2)$ above ~150 °C when either $k_a$ or $k_b$ is used for the $(e_{aq}^- + e_{aq}^-)$ reaction rate constant.

## 4. Conclusion

In this work, Monte Carlo simulations were used to calculate the *G*-values for the primary species of the radiolysis of neutral liquid water and 0.4 M $H_2SO_4$ aqueous solutions by the recoil ions of the $^{10}B(n,\alpha)^7Li$ nuclear reaction at temperatures between 25 and 350 °C. Overall, the simulation results for neutral deaerated water agreed well with existing estimates at 20 and 289 °C. For 0.4 M $H_2SO_4$ solutions, reasonable agreement between experiment and simulation was also found at room temperature. Compared with the data obtained for low-LET radiation, our computed yields showed essentially similar temperature dependences over the range of temperatures studied, but with lower values for yields of free radicals and higher values for molecular yields, which reflect the high-LET character of the densely ionizing $^{10}B(n,\alpha)^7Li$ recoil ions. More experimental data are required for both neutral and acidic solutions to better describe the dependence of radiolytic yields on temperature and to test our modeling calculations more thoroughly. Moreover, measurements of the $(e_{aq}^- + e_{aq}^-)$ reaction rate constant in near-neutral water would help us to determine whether the predicted non-monotonic inflections above ~150 °C in $G(H_2)$ and $G(H_2O_2)$ are confirmed.

## Acknowledgements

The authors thank Professor Takayuki Terai, Professor Yusa Muroya, and Dr Shin-ichi Yamashita for their support and advices. They are also grateful to Professor James F. Ziegler for his helpful correspondence with regard to the use of the SRIM simulation software. M. M. I. is the recipient of a scholarship from the "Centre de Recherche Médicale de l'Université de Sherbrooke". P. L. thanks the Ministry of Education, Culture, Sports, Science, and Technology (MEXT) of Japan for financial support through a MEXT scholarship. The research of J.-P. J.-G. is supported by the Natural Sciences and Engineering Research Council of Canada (NSERC) Grant No. RGPIN-2015-06100.

## Notes and references

1 *Neutron Capture Therapy. Principles and Applications*, ed. W. A. G. Sauerwein, A. Wittig, R. Moss and Y. Nakagawa, Springer, Berlin, 2012.

 

2 G. F. Knoll, *Radiation Detection and Measurement*, Wiley, New York, 3rd edn, 2000, p. 507.
3 D. E. Watt, *Quantities for Dosimetry of Ionizing Radiations in Liquid Water*, Taylor & Francis, London, 1996.
4 É. Sèche, R. Sabattier, J.-C. Bajard, G. Blondiaux, N. Breteau, M. Spotheim-Maurizot and M. Charlier, *Radiat. Res.*, 2002, **158**, 292.
5 N. S. Hosmane, J. A. Maguire, Y. Zhu and M. Takagaki, *Boron and Gadolinium Neutron Capture Therapy for Cancer Treatment*, World Scientific, Singapore, 2012.
6 G. L. Locher, *Am. J. Roentgenol. Radium Ther.*, 1936, **36**, 1.
7 J. Chadwick, *Proc. R. Soc. London, Ser. A*, 1932, **136**, 692.
8 P. G. Kruger, *Proc. Natl. Acad. Sci. U. S. A.*, 1940, **26**, 181.
9 W. Sauerwein, *Strahlenther. Onkol.*, 1993, **169**, 1.
10 J. W. Hopewell, G. M. Morris, A. Schwint and J. A. Coderre, *Appl. Radiat. Isot.*, 2011, **69**, 1756.
11 R. F. Barth, M. G. H. Vicente, O. K. Harling, W. S. Kiger III, K. J. Riley, P. J. Binns, F. M. Wagner, M. Suzuki, T. Aihara, I. Kato and S. Kawabata, *Radiat. Oncol.*, 2012, **7**, 146.
12 R. L. Moss, *Appl. Radiat. Isot.*, 2014, **88**, 2.
13 J. Pucheault, M. Lefort and M. Haïssinsky, *J. Chim. Phys. Phys.–Chim. Biol.*, 1952, **49**, 286.
14 M. Koike, E. Tachikawa and T. Matsui, *J. Nucl. Sci. Technol.*, 1969, **6**, 163.
15 P. Cohen, *Water Coolant Technology of Power Reactors*, American Nuclear Society, La Grange Park, 1980.
16 J. Takagi, B. J. Mincher, M. Yamaguchi and Y. Katsumura, in *Charged Particle and Photon Interactions with Matter: Recent Advances, Applications, and Interfaces*, ed. Y. Hatano, Y. Katsumura and A. Mozumder, Taylor & Francis Group, Boca Raton, 2011, p. 959.
17 E. J. Hart, W. R. McDonell and S. Gordon, *Proceedings of the International Conference on the Peaceful Uses of Atomic Energy, Geneva, 8-20 Aug. 1955, P/839*, United Nations, New York, 1956, vol. 7, p. 593.
18 D. R. McCracken, K. T. Tsang and P. J. Laughton, *Aspects of the physics and chemistry of water radiolysis by fast neutrons and fast electrons in nuclear reactors, Report AECL-11895*, Atomic Energy of Canada Limited, Chalk River, Ontario, 1998.
19 H. Christensen, *Fundamental aspects of water coolant radiolysis, SKI Report 2006:16*, Swedish Nuclear Power Inspectorate, Stockholm, Sweden, April 2006.
20 A. J. Elliot and D. M. Bartels, *The reaction set, rate constants and g-values for the simulation of the radiolysis of light water over the range 20° to 350 °C based on information available in 2008*, Report AECL No. 153-127160-450-001, Atomic Energy of Canada Limited, Chalk River, Ontario, 2009.
21 R. L. Cowan, *Water Chemistry of Nuclear Reactor Systems 7, Bournemouth, UK, 13-17 Oct. 1996*, British Nuclear Energy Society, London, 1996, p. 196.
22 Y. Wada, A. Watanabe, M. Tachibana, K. Ishida, N. Uetake, S. Uchida, K. Akamine, M. Sambongi, S. Suzuki and K. Ishigure, *J. Nucl. Sci. Technol.*, 2001, **38**, 183.
23 N. F. Barr and R. H. Schuler, *Radiat. Res.*, 1957, **7**, 302; N. F. Barr and R. H. Schuler, *J. Phys. Chem.*, 1959, **63**, 808.
24 M. Lefort, *Annu. Rev. Phys. Chem.*, 1958, **9**, 123.
25 J. Pucheault and P. Sigli, *Int. J. Radiat. Phys. Chem.*, 1976, **8**, 613; see also P. Sigli, Ph.D. thesis, Université Paris VI, Paris, 1972.
26 P. Lertnaisat, Y. Katsumura, J. Meesungnoen, J.-P. Jay-Gerin, S. Mukai, R. Umehara, Y. Shimizu and M. Suzuki, *15th International Congress of Radiation Research*, Kyoto, Japan, 25–29 May 2015, Poster 2-PS6D-06.
27 J. Meesungnoen and J.-P. Jay-Gerin, *J. Phys. Chem. A*, 2005, **109**, 6406.
28 J. Meesungnoen and J.-P. Jay-Gerin, in *Charged Particle and Photon Interactions with Matter: Recent Advances, Applications, and Interfaces*, ed. Y. Hatano, Y. Katsumura and A. Mozumder, Taylor & Francis Group, Boca Raton, 2011, p. 355; see also J. Meesungnoen, Ph.D. thesis, Université de Sherbrooke, Sherbrooke, Québec, Canada, 2007.
29 S. Sanguanmith, Y. Muroya, J. Meesungnoen, M. Lin, Y. Katsumura, L. Mirsaleh Kohan, D. A. Guzonas, C. R. Stuart and J.-P. Jay-Gerin, *Chem. Phys. Lett.*, 2011, **508**, 224.
30 J. Meesungnoen, S. Sanguanmith and J.-P. Jay-Gerin, *RSC Adv.*, 2015, **5**, 76813.
31 R. L. Platzman, in *Radiation Biology and Medicine. Selected Reviews in the Life Sciences*, ed. W. D. Claus, Addison-Wesley, Reading, 1958, p. 15.
32 M. Tachiya, *Radiat. Phys. Chem.*, 1983, **21**, 167.
33 S. M. Pimblott, M. J. Pilling and N. J. B. Green, *Radiat. Phys. Chem.*, 1991, **37**, 377.
34 Y. Frongillo, T. Goulet, M.-J. Fraser, V. Cobut, J. P. Patau and J.-P. Jay-Gerin, *Radiat. Phys. Chem.*, 1998, **51**, 245.
35 T. Goulet, M.-J. Fraser, Y. Frongillo and J.-P. Jay-Gerin, *Radiat. Phys. Chem.*, 1998, **51**, 85.
36 I. Plante, Ph.D. thesis, Université de Sherbrooke, Sherbrooke, Québec, Canada, 2009.
37 N. Autsavapromporn, J. Meesungnoen, I. Plante and J.-P. Jay-Gerin, *Can. J. Chem.*, 2007, **85**, 214.
38 T. Tippayamontri, S. Sanguanmith, J. Meesungnoen, G. R. Sunaryo and J.-P. Jay-Gerin, *Recent Res. Dev. Phys. Chem.*, 2009, **10**, 143.
39 J. F. Ziegler, J. P. Biersack and M. D. Ziegler, *SRIM - The Stopping and Range of Ions in Matter*, SRIM Co., Chester, MD, 2015; see also J. F. Ziegler, M. D. Ziegler and J. P. Biersack, *Nucl. Instrum. Methods Phys. Res., Sect. B*, 2010, **268**, 1818.
40 J. A. LaVerne, in *Charged Particle and Photon Interactions with Matter: Chemical, Physicochemical, and Biological Consequences with Applications*, ed. A. Mozumder and Y. Hatano, Marcel Dekker, New York, 2004, p. 403.
41 S. Gordon, K. H. Schmidt and J. R. Honekamp, *Radiat. Phys. Chem.*, 1983, **21**, 247.
42 J. Meesungnoen, J.-P. Jay-Gerin, A. Filali-Mouhim and S. Mankhetkorn, *Radiat. Res.*, 2002, **158**, 657.
43 A. O. Allen, *The Radiation Chemistry of Water and Aqueous Solutions*, D. Van Nostrand Co., Princeton, NJ, 1961.
44 S. Sanguanmith, J. Meesungnoen, Y. Muroya, M. Lin, Y. Katsumura and J.-P. Jay-Gerin, *Phys. Chem. Chem. Phys.*, 2012, **14**, 16731.

45 D. Swiatla-Wojcik and G. V. Buxton, *J. Phys. Chem.*, 1995, **99**, 11464.
46 M.-A. Hervé du Penhoat, T. Goulet, Y. Frongillo, M.-J. Fraser, Ph. Bernat and J.-P. Jay-Gerin, *J. Phys. Chem. A*, 2000, **104**, 11757.
47 S. L. Butarbutar, Y. Muroya, L. Mirsaleh Kohan, S. Sanguanmith, J. Meesungnoen and J.-P. Jay-Gerin, *At. Indones.*, 2013, **39**, 51.
48 S. L. Butarbutar, S. Sanguanmith, J. Meesungnoen, G. R. Sunaryo and J.-P. Jay-Gerin, *Radiat. Res.*, 2014, **181**, 659.
49 S. Sanguanmith, J. Meesungnoen, D. A. Guzonas, C. R. Stuart and J.-P. Jay-Gerin, *J. Nucl. Eng. Radiat. Sci.*, 2016, **2**, 021014.
50 A. J. Elliot, *Rate constants and g-values for the simulation of the radiolysis of light water over the range 0-300 °C, Report AECL-11073*, Atomic Energy of Canada Limited, Chalk River, Ontario, 1994.
51 C. R. Stuart, D. C. Ouellette and A. J. Elliot, *Pulse radiolysis studies of liquid heavy water at temperatures up to 250 °C, Report AECL-12107*, Atomic Energy of Canada Limited, Chalk River, Ontario, 2002.
52 D. Hatomoto, Y. Muroya, Y. Katsumura, S. Yamashita and T. Kozawa, in *Book of Abstracts, 5th Asia-Pacific Symposium on Radiation Chemistry, University of Tokyo*, Tokyo, Japan, 8–11 Sept. 2014, Paper No. P08, p. 140.
53 S. Sanguanmith, Y. Muroya, T. Tippayamontri, J. Meesungnoen, M. Lin, Y. Katsumura and J.-P. Jay-Gerin, *Phys. Chem. Chem. Phys.*, 2011, **13**, 10690.
54 C. D. Alcorn, J.-C. Brodovitch, P. W. Percival, M. Smith and K. Ghandi, *Chem. Phys.*, 2014, **435**, 29.
55 C. Ferradini and J.-P. Jay-Gerin, *Res. Chem. Intermed.*, 2000, **26**, 549.

 